

## Evaluation of M4 ocean tide loading inside the GGP network

Ducarme Bernard<sup>1</sup>, Zhou Jiangcun<sup>2</sup>, Sun Heping<sup>2</sup>

<sup>1</sup> Research Associate NFSR, Royal Observatory of Belgium, Av. Circulaire 3, B-1180 Brussels, Belgium.

<sup>2</sup> Institute of Geodesy and Geophysics, Chinese Academy of Sciences, 340 Xu Dong road, 430077 Wuhan, China.

### Abstract

The determination of M4 from tidal gravity records is not a trivial problem. The amplitude at the equator does not exceed 27 nanogal ( $1\text{ngal}=10^{-11}\text{m.s}^{-2}$ ) and drops to 6.7 nanogal at a latitude of  $45^\circ$ . Quarter-diurnal (QD) spectrum has been accurately determined in the superconducting gravimeters (SG) records using the new VAV tidal analysis program. Recently the FES04 ocean tides model provided a world map for M4. The worldwide distribution of Global Geodynamics Project (GGP) stations equipped with SG's provides a good opportunity to check the capacity of this model to provide reliable tidal loading estimations. The West European area with its concentration of SG observations and several local models available for M4 is the best test area. Tidal loading on M4 frequency is still important at several hundred kilometres inside the continent. In Europe the results for M4 points clearly to a better efficiency of the tidal loading corrections computed using the Pingree & Griffiths model. The final residue reaches the level of 1ngal only for stations beyond  $10^\circ$  of East longitude. Reasonable tidal factors are obtained in stations (Boulder and Wuhan), where the loading is weak and the theoretical amplitude at the level of 10 ngal. It means that instrumental nonlinearities are not producing spurious signals at M4 frequency. Generally however the M4 tide included in the ocean model FES04 does not provide efficient tidal loading corrections for tidal gravity observations.

**Keywords:** non-linear tides, superconducting gravimeter, GGP

### 1. Introduction

Quarter-diurnal (QD) spectrum has been clearly identified in the superconducting gravimeters (SG) records since a long time (Florsch et al., 1995). The main QD non linear tides due to ocean tides loading are present in the stacking of SG data used for the identification of the Slichter's modes (Sun et al., 2003, 2004). It should thus be important to be able to suppress these non-linear tides from the residues at the level of the tidal analysis. It is now possible using the VAV tidal analysis software (Venedikov et al., 2003, 2005; Ducarme et al., 2006).

The recent FES04 ocean tides model ([/pub/soa/mare/tide\\_model/global\\_solution/fes2004/tide/](/pub/soa/mare/tide_model/global_solution/fes2004/tide/) at <ftp.legos.obs-mip.fr>) is providing a global map for the quarter-diurnal wave M4, which is the main QD non-linear tidal constituent. Its amplitude can be large on the continental shelf, typically along the European coast from the Gulf of Biscay to the North Sea or on the Patagonian shelf. The worldwide distribution of GGP stations (Fig. 1-3, Crossley et al., 1999, <http://www.eas.slu.edu/GGP/ggpmaps.html>), equipped with superconducting

gravimeters (SG), is a good opportunity to check the capacity of this model to provide reliable tidal loading estimations. The West European area with its concentration of SG observations and several local models available for M4 is the best test area. However the determination of M4 from tidal gravity records is not a trivial problem. The amplitude at the equator does not exceed 27 nanogal ( $1\text{ngal}=10^{-11}\text{m.s}^{-2}$ ) and drops to 6.7 nanogal at a latitude of  $45^\circ$ . Moreover several non linear tides, which are not existing in the tidal potential, are generated in the shallow waters: “shallow water tides” (SWT) (Boy et al., 2004).

As M2 is one of the main tidal constituents in the astronomical tides, any non-linearity in the sensor and its electronics will produce a spurious M4 wave mixing up with the true tidal gravity wave and the indirect effect of the ocean tide. Other non-linear tides can be created also in a way similar to the shallow water constituents. As all the SGs have a similar design we could have a systematic effect. It is thus important to find in the GGP network stations with very low ocean tide loading for M4 and check if the tidal parameters obtained in such places are close to the models of response of the Earth to the tidal potential of degree four.

In this paper we shall first discuss the optimisation of the determination of the M4 tide in the tidal gravity records and then compare our results with several ocean tides models in Europe and with FES04 alone in the rest of the world.

## 2. Quarter-diurnal spectrum

The spectrum of the quarter-diurnal waves coming from the potential of degree 4 order 4 is limited to a few main constituents (Table 1, Tamura, 1987).

Table 1: Main tidal components from the  $W_4^4$  potential according to Tamura, 1987  
Amplitudes are given in nanogal ( $10^{-11}\text{m.s}^{-2}$ )

Wave	Angular speed °/h	Doodson number	Amplitude at $\varphi=45^\circ$
N4	56.87945907	435.755	0.52
3MS4	56.95231272	437.555	0.46
MN4	57.42383377	445.655	2.40
2MLS4	57.49668743	447.455	0.46
M4	57.96820848	455.555	6.69
ML4	58.51258319	465.455	0.28
KN4	58.52186681	465.655	0.57
MK4	59.06624152	475.555	1.18

The amplitudes are four times bigger at the equator as the dependence is in  $\cos^4\varphi$ . Besides M4 one will notice its two elliptic waves MN4 and ML4. The groups can be separated on one month, except for (N4,3MS4) and (MN4,2MLS4). For these groups 6 months are required. ML4 and KN4 form a single group that can be separated on 4 years, as their arguments differ only by two times the lunar perigee argument.

It should be noted that, with long SG records, the RMS error is at the level of 0.2ngal ( $210^{-12}\text{ms}^{-2}$ ) in amplitude, in the best signal to noise conditions, and is

generally close to 0.4ngal. In such conditions it is very difficult to determine precise tidal factors for waves below  $1\text{mms}^{-2}$  and one should limit the tidal separation to the three main constituents MN4 (group 435-447), M4 (group 455) and MK4 (group 465-475).

On the other hand, 18 non-linear tides (SWT) identified in the GGP SG records, are listed in table 2. These terms do not always coincide with waves identified in the tidal potential.

It should be noted that the main wave M4 is surrounded by the semi-annual modulations  $\pm |S2-K2|$ , corresponding to an annual amplitude modulation of the constitutive semi-diurnal terms. For example 2MSK4 is equivalent to  $\alpha_4$  and 2MKS4 to  $\beta_4$ . These last waves have not been observed with SG, except in Sutherland.

Table 2: non-linear tides (shallow water components) observed in the SG records

Wave	generation	Angular speed °/h
2MNS4	2*M2+N2-S2	56.40793843
•N4	N2*N2	56.87945907
2MvS4	2*M2+v2-S2	56.48079200
N4	2*N2	56.87945906
•3MS4	3*M2-S2	56.95231272
MSNK4	M2+S2+N2-K2	57.34169649
•MN4	M2+N2	57.42383377
Mv4	M2+v2	57.49668743
2MSK4	2*M2+(S2-K2)	57.88607120
•M4	2*M2	57.96820848
2MKS4	2*M2+(K2-S2)	58.05034576
SN4	S2+N2	58.43972953
•KN4	K2+N2	58.52186681
MT4	M2+T2	58.94303756
MS4	M2+S2	58.98410424
•MK4	M2+K2	59.06624152
SL4	S2+L2	59.52847895
*S4	S2*S2	60.00000000
SK4	S2+K2	60.08213278

\* from meteorological origin

• already present in the tidal potential

From these considerations we can derive three possible ways for the determination of M4 in tidal records:

- Separate the three main tidal groups MN4, M4 and MK4, without introduction of additional non linear tides;
- Introduce non linear tides only (shallow only solution);

- Put all tidal waves coming from the potential in one single M4 group and introduce selected additional non linear tides. These terms will take into account the difference between the tidal factor at each perturbed frequency and the tidal factors of M4.

The VAV tidal analysis method provides an easy way to select the optimal solution through the “Akaike Criterion” (AIC, Sakamoto et al., 1986). For different computations using the same data set and different unknowns the best solution corresponds to a minimum value of AIC.

The use of AIC coupled with a  $3\sigma$  signification test allows also the selection of the SWT really present in any tidal record. As example we show below two correction steps at Sutherland. In Figure 1 the spectrum of the original data is compared with the tidal potential, showing a large SWT (MS4), not existing in the Tamura potential, as well as the meteorological wave S4. In figure 2 the major components have been eliminated (AIC=6231). A few spectral peaks are still visible i.e. from left to right two side waves of MN4, MT4 and several side lobes of S4. These last spectral peaks correspond to the annual and semi-annual modulations of the meteorological wave S4. After elimination of 11 components significant at the  $3\sigma$  level and of the meteorological waves the final spectrum is nearly flat (AIC=5948). A similar approach is possible in any tidal band. It is thus possible to clean individually all the GGP stations records before the application of sophisticated detection methods for the detection of the Slichter modes or any core mode.

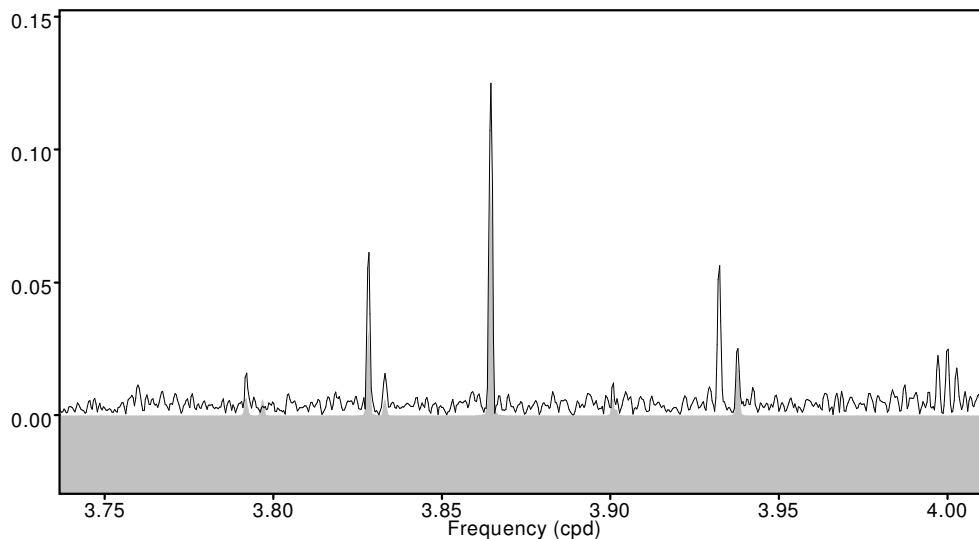


**Figure 1:** Spectrum at Sutherland: residues (full line) and tidal potential (shaded)

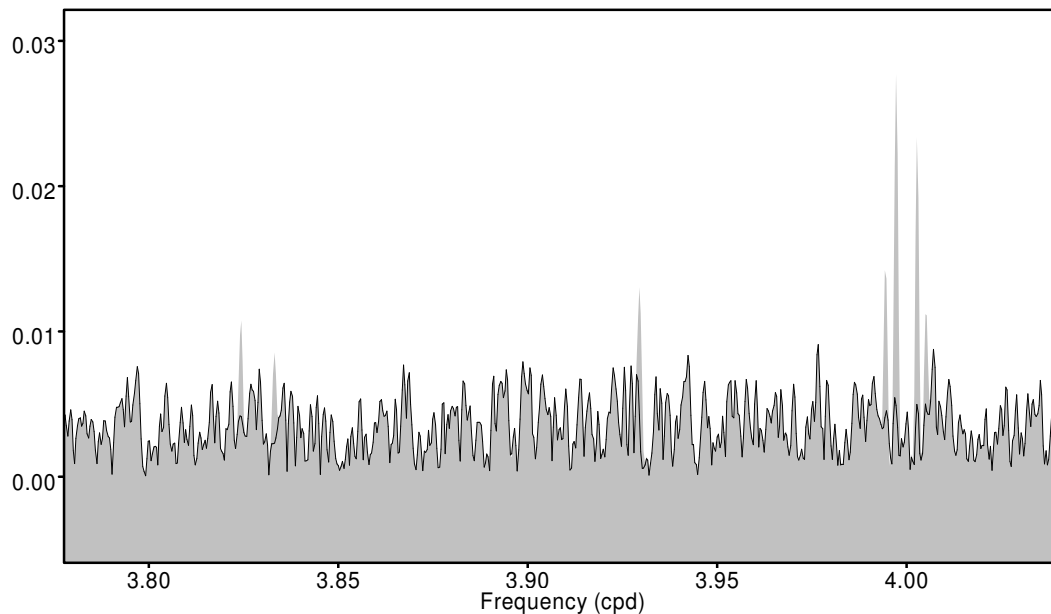


**Figure 2:** improved gravity residues at Sutherland : first elimination step (shaded) and final (full line)

### 3. Detection of the quarter-diurnal tides by the GGP network (Table 3)

The “shallow only” solution does never correspond to the optimal one, except when the amplitude of the astronomical tide is very weak as in Ny Alesund (NY) and Syowa (SY). In these stations all the observed QD tides are purely non-linear ones. The solution with the tidal potential alone was optimal in two stations only (BO and WU), where only one shallow water tide is significant (Table 3). A maximum of 11 significant non linear terms, including  $\alpha_4$  and  $\beta_4$  was found in Sutherland (SU) (Figure 1). The pure non-linear tides terms MS4 and SK4 are observed in 15 stations among 21. In Europe a maximum of 10 non linear tides are observed in Moxa (MO). The number of observed terms depends in a critical way from the signal to noise ratio, which is very high in MO, and from the distance to the sea. We observe only 4 terms in Vienna (VI) (Figure 2), where the data quality is the same. A higher number of non linear terms are observed in Medicina (MC), probably due to the vicinity of the Adriatic Sea.

A general conclusion is that quarter-diurnal non linear terms are present in gravity records even far from the coast. It is a reason why they were found in the stacking of tidal gravity records used for the detection of the Slichter modes (Sun et al., 2003, 2004).

Table 3: Quarter-diurnal tides detected by the GGP network

N: number of observed non-linear tides

Theoretical ( $A_{th}$ ) and observed ( $A_o$ ) amplitudes are in  $ngal (10^{-11} nms^{-2})$

MSD: mean square deviation of the unit weight in  $ngal (10^{-11} nms^{-2})$

Stations are listed by order of increasing M4 amplitude from poles to equator

Station		M4*		MN4*	MS4	MK4*	SK4	N	MSD
		$A_{th}$	$A_o$	$A_o$	$A_o$	$A_o$	$A_o$		
Ny Alesund	NY	0.04	24.89±1.46	10.16	9.20	5.20	2.33	6	180
Syowa	SY	0.44	29.86±0.88	14.92	12.07	3.30	4.13	10	96
Metsahovi	ME	1.63	0.29±0.36	-	1.08	0.81	-	3	68
Potsdam	PO	3.72	1.57±0.44	1.04	1.42	-	1.63	3	66
Brussels	BE	4.28	4.09±0.55	2.44	3.67	1.45	-	4	136
Moxa	MO	4.33	1.25±0.20	1.10	1.00	0.89	1.12	10	40
Membach	MB	4.35	2.08±0.26	2.08	2.02	0.81	-	4	52
Bad Homburg	BA	4.49	1.42±0.28	2.47	1.80	1.27	1.17	6	53
Wetzell	WE	4.91	1.63±0.20	1.51	1.59	0.41	1.35	5	45
Strasbourg	ST	5.12	2.34±0.23	2.64	2.81	1.08	0.89	7	41
Vienna	VI	5.27	2.51±0.23	0.87	1.17	0.89	0.73	4	39
Cantley	CA	6.43	4.98±0.36	1.45	1.05	1.05	0.74	6	73
Medicina	MC	6.93	2.73±0.27	1.84	3.55	1.10	1.33	8	46
Boulder	BO	9.16	10.24±0.41	1.54	-	-	-	1	67
Esashi	ES	9.69	11.91±1.44	8.13	3.49	2.80	3.45	4	203
Tigo/Concepc.	TC	10.99	15.59±0.72	8.27	2.18	2.53	1.22	6	73
Matsushiro	MA	11.17	10.59±0.45	2.34	1.55	-	2.19	4	66
Canberra	CB	11.88	17.37±0.29	1.42	4.25	0.82	1.63	7	52
Sutherland	SU	13.63	33.87±0.34	6.60	8.85	3.81	0.99	11	60
Wuhan	WU	14.76	15.54±0.41	-	-	1.07	-	1	61
Bandung	BA	26.00	21.64±0.94	4.53	14.01	3.91	-	6	93

\* quarter-diurnal wave present in the tidal potential

#### 4. Updated results for M4 in Europe

The different tidal vectors (**A**, **R**, **L**, **B**, **X**), used below, are described in Figure 3. In a recent paper Boy et al. (2004) tried to model the ocean tides loading in West Europe for the tidal wave M4 using different ocean tides models (Mog2D, Pingree and Griffiths, 1980 and Flather, 1976), covering the English channel, the gulf of Biscay, the North sea, the Irish sea and the North Atlantic. The authors compare directly the “observed non-linear tidal loading” (OTL) vector obtained in 8 European GGP stations (Table 2 in Boy et al., 2004) with the computed ocean load vector  $L(L,\lambda)$  (Table 5 in Boy et al., 2004). The phase of the load vector with respect to Greenwich is quite homogeneous from Strasbourg to Vienna (Table 4). The behaviour of the station Metsahovi (ME) is different and it is not surprising as it is geographically separated from the other European stations and close to the Gulf of Finland. The most recent model Mog2D is giving load vector amplitudes

which are twice as large as the OTL vectors (**B** in Table 5), while Pingree & Griffith model is closer to the observations. The phase agreement of these two models with the observations is very good for inland stations (Brussels, Membach and Metsahovi) excluded, while Flather's model displays a strong phase bias. This last model is not displayed in Table 4.

Table 4: Tidal loading computation for M4 in Europe  
Amplitudes are given in ngal ( $10^{-11} \text{ nms}^{-2}$ )  
Greenwich phase in degrees and oceanographic convention

Station	Residue		FES04		Pingree&Griffiths		Mog2D	
	<b>B</b>		<b>L</b>		<b>L*</b>		<b>L*</b>	
	B	$\beta$	L	$\lambda$	L	$\lambda$	L	$\lambda$
	<i>RMS</i>							
BE	4.65	215.8	3.5	121.2	4.0	266.8	8.8	94.4
Brussels	$\pm 55$	$\pm 7.7$						
MB	3.88	183.2	3.4	151.7	4.3	217.8	9.0	122.0
Membach	$\pm 26$	$\pm 7.3$						
ST	7.64	147.9	5.5	180.6	4.9	158.9	11.4	141.4
Strasbourg	$\pm 23$	$\pm 5.7$						
MO	3.61	146.1	3.9	176.9	3.4	147.6	7.3	142.9
Moxa	$\pm 20$	$\pm 9.0$						
WE	4.56	146.8	3.4	178.9	3.4	152.8	7.0	142.8
Wetzell	$\pm 20$	$\pm 7.1$						
PO	2.31	131.4	3.1	169.1	3.1	138.3	6.6	147.0
Potsdam	$\pm 44$	$\pm 16.1$						
VI	3.54	135.4	2.5	181.6	2.9	152.2	5.5	142.8
Vienna	$\pm 23$	$\pm 5.2$						
ME	1.96	78.7	3.1	130.2	2.7	137.0	3.5	163.3
Metsahovi	$\pm 36$	$\pm 7.0$						

\* taken from Table 5 in Boy et al., 2004

In this study we compute first the tidal loading vector **L** at the same sites using the FES04 model (Table 4, Figure 4). The tidal loading vector **L**, which takes into account the direct attraction of the water masses, the flexion of the ground and the associated change of potential, was evaluated by performing a convolution integral between the ocean tide models and the load Green's function computed by Farrell (Farrell, 1972). To compute the residual vector **B**(**B**, $\beta$ ) we subtracted from the observed amplitude vector **A**(**A**, $\alpha$ ), the body tide response **R**( $\delta_{th}$  **A**<sub>th</sub>,0), using a theoretical amplitude factor  $\delta_{th}= 1.038$  corresponding to the  $W_4^4$  tidal potential (Dehant et al., 1999). The theoretical amplitude is given for each station in Table 5. This **B** vector should be compared with the OTL vector in Boy et al., 2004. However we used longer time series than these authors.

There is a systematic phase difference of the order of 30° to 40° between the load computations using Mog2D and FES04. The amplitude L computed by Mog2D is

twice the amplitude deduced from FES04, which in turn is close to Pingree & Griffiths.

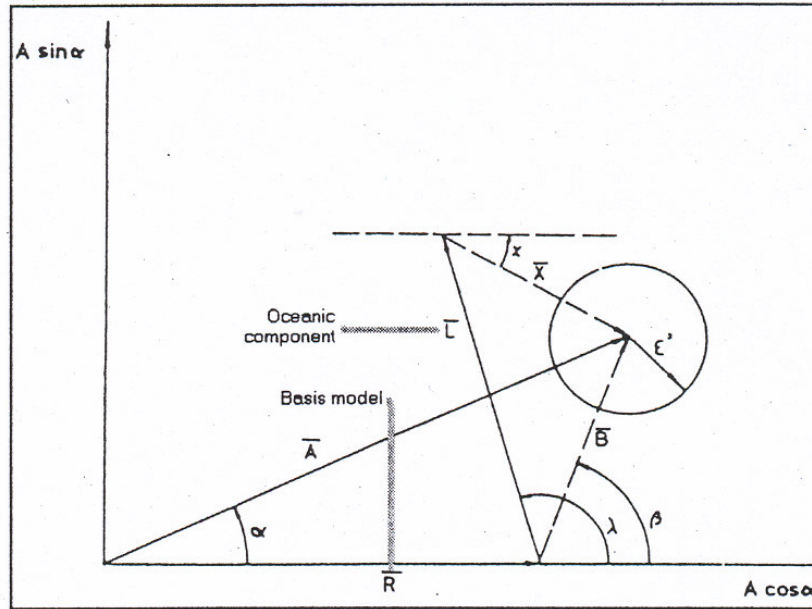


**Figure 3:** Relationship between the observed tidal amplitude vector  $\mathbf{A}(A,\alpha)$ , the Earth model  $\mathbf{R}(R,0)$ , the computed ocean tides load vector  $\mathbf{L}(L,\lambda)$ , the tidal residue  $\mathbf{B}(B,\beta) = \mathbf{A} - \mathbf{R}$  and the corrected residue  $\mathbf{X}(X,\chi) = \mathbf{B} - \mathbf{L}$ .

The residual vector (Table 4, Figure 4) agrees within the RMS errors with the OTL vector given in the table 2 of Boy et al, 2004. It shows that the results of the data analysis are very stable. Obviously Pingree & Griffiths model is the only one able to recover the strong phase decrease between BE and ST and the amplitude of the load vectors is always close to the observed residue  $\mathbf{B}$ . FES04 is predicting correctly the amplitudes but its phases are always too large from Strasbourg (ST) to Vienna (VI). On the contrary, the phases of Mog2D are generally in good agreement with the observations, while the amplitudes are much too large.

Table 5 displays the final residue

$$\mathbf{X}(X,\chi) = \mathbf{B}(B,\beta) - \mathbf{L}(L,\lambda),$$

which represents the unexplained part of the residual vector after correction using the Pingree & Griffiths model. One notices a strong diminution for the central European stations (MO, WE, PO, VI) and a diminution by a factor of two in ST, but a slight improvement only for BE and MB. Obviously no model is able to represent correctly the tidal loading at M4 frequency for stations with longitude less than  $10^\circ$ .

As a conclusion, we cannot really trust the M4 ocean tide correction extracted from the FES04 model in Europe, due probably to a still too coarse grid.



Table 5: Tidal residues for M4 in Europe corrected with Pingree & Griffiths map

$A_{th}$ : theoretical amplitude for M4,  $\sigma$ : RMS error

Amplitudes are given in  $ngal$  ( $10^{-11}nms^{-2}$ )

Greenwich phase in degrees and oceanographic convention

Station	Residue <b>B</b>		Final Residue <b>X</b>		$A_{th}$	Pingree & Griffiths <b>L*</b>	
	B	$\beta$	X	$\chi$		L	$\lambda$
	$\sigma$	$\sigma$					
BE	4.65	215.8	3.76	160.3	4.3	4.0	266.8
Brussels	$\pm 5.5$	$\pm 7.7$					
MB	3.88	183.2	2.45	101.7	4.4	4.3	217.8
Membach	$\pm 2.6$	$\pm 7.3$					
ST	7.64	147.9	3.00	180.6	5.1	4.9	158.9
Strasbourg	$\pm 2.3$	$\pm 5.7$					
MO	3.61	146.1	0.28	127.3	4.3	3.4	147.6
Moxa	$\pm 2.0$	$\pm 9.0$					
WE	4.56	146.8	1.22	129.7	4.9	3.4	152.8
Wetzell	$\pm 2.0$	$\pm 7.1$					
PO	2.31	131.4	0.83	-22.1	3.7	3.1	138.3
Potsdam	$\pm 4.4$	$\pm 16.1$					
VI	3.54	135.4	1.14	88.8	5.3	2.9	152.2
Vienna	$\pm 2.3$	$\pm 5.2$					
ME	1.96	78.7	2.39	1.4	1.6	2.7	137.0
Metsahovi	$\pm 3.6$	$\pm 7.0$					

\* taken from Table 5 in Boy et al., 2004

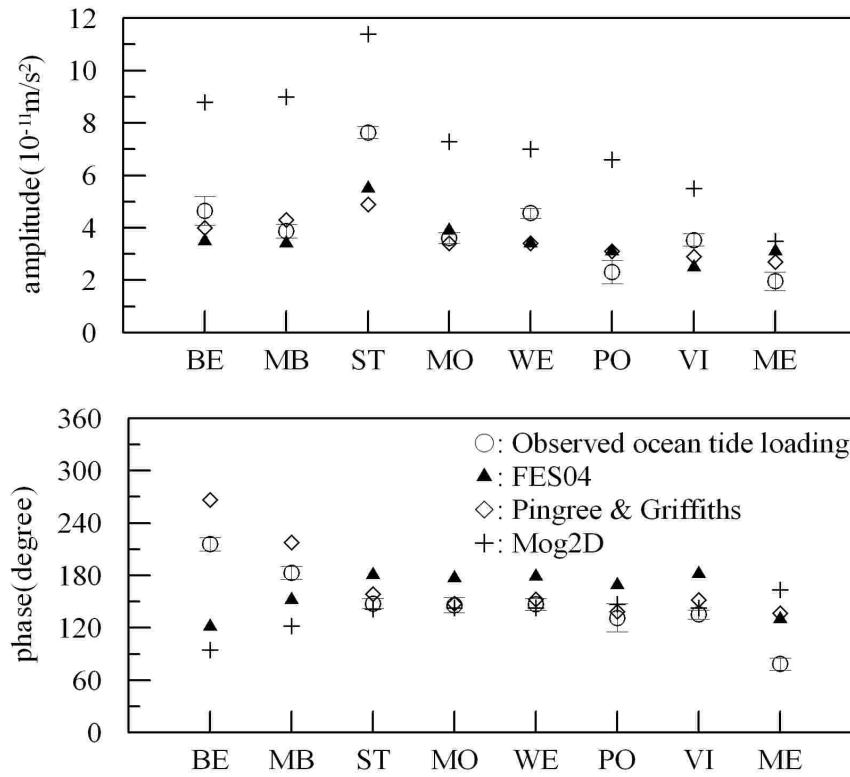


**Figure 4:** Observed residue (**B**) and computed (**L**) ocean tide loading vectors for three different models

## 5. Results for the rest of the world

We are mainly interested by two different situations:

- stations with a weak loading where we can directly observe the body tides if the theoretical amplitude is not too weak;
- stations with a large tidal loading where we can test the efficiency of the tidal loading corrections, especially when the body tides are weak.

Table 6: Tidal factors at Boulder (BO) and Wuhan (WU)

L is the amplitude of the tidal loading vector and  $\sigma$  the RMS error

Station	$A_{th}$ ngal	Observed		Corrected		L ngal
		$\delta_o$	$\alpha_o$ ( $^\circ$ )	$\delta_c$	$\alpha_c$ ( $^\circ$ )	
		$\sigma$	$\sigma$			
Boulder (BO)	9.2	1.1147	-0.954	1.1063	0.086	0.2
		$\pm 0.447$	$\pm 2.297$			
Wuhan (WU)	14.8	1.0519	-1.648	1.0984	-3.748	0.9
		$\pm 0.275$	$\pm 1.496$			

In the first category we can only select BO and WU, where the tidal loading is smaller than one nanogal and the astronomical amplitude reaches 10 ngal.

Here we introduce explicitly the observed ( $\delta_o$ ) and corrected ( $\delta_c$ ) amplitude factors. The corrected vector  $\mathbf{A}_c(\delta_c A_{th}, \alpha_c)$  is given as

$$\mathbf{A}_c = \mathbf{A}_o(\delta_o A_{th}, \alpha) - \mathbf{L}(L, \lambda)$$

The results are quite good as seen from Table 6. The corrected amplitude factor is a bit too large with respect to the theoretical value  $\delta_{th} = 1.038$ , but the discrepancy is still within the two sigma range. The phase differences do not differ significantly from zero. In WU the observed factor is closer to the theoretical value than the corrected one, while the tidal loading is negligible in BO. Obviously, the tidal loading correction computed from the FES04 map does not improve the results. In any case instrumental nonlinearities are not producing spurious signals at M4 frequency.

Table 7: Tidal residues for M4 corrected with FES04

$A_{th}$ : theoretical amplitude for M4,  $\sigma$ : RMS error

MSD: mean square deviation of the unit weight from VAV

Amplitudes are given in ngal ( $10^{-11} \text{ nms}^{-2}$ )

Greenwich phase in degrees and oceanographic convention

Station name	Residue		Final Residue		$A_{th}$	FES04	
	B	$\beta$	X	$\chi$		L	$\lambda$
<i>MSD</i>	$\sigma$	$\sigma$					
Cantley (CA)	3.0	80	1.9	73	6.4	1.1	91
60	$\pm 4$	$\pm 4$					
Esashi (ES)	9.2	51	7.6	49	9.7	1.6	61
203	$\pm 1.4$	$\pm 7$					
Tigo (TC)	12.4	-165.0	15.5	-142	11.0	6.4	88
73	$\pm 7$	$\pm 3$					
Matsushiro (MA)	8.4	48	4.2	53	11.2	4.2	44
66	$\pm 5$	$\pm 2$					
Canberra (CB)	7.5	64	7.6	11	11.9	6.7	129
52	$\pm 3$	$\pm 1$					
Sutherland (SU)	19.9	-98	14.3	-131	13.7	11.1	-53
60	$\pm 3$	$\pm 1$					
Bandung (BA)	16.5	163	12.4	151	26.0	5.1	194
93	$\pm 9$	$\pm 2$					

Among the stations with a large tidal loading we should reject coastal stations as the grid of FES04 is not fine enough. It is the case for NY and SY.

In most of the stations of Table 7, the correction does not reduce the observed residue. However the residual vector is divided by a factor of two if in Cantley (CA) and Matsushiro (MA). In Esashi (ES) the phases  $\lambda$  (load vector) and  $\beta$  (residual vector) agree but the amplitude  $L$  of the tidal loading vector is too weak. The phase of the load should be reduced of  $30^\circ$  in Bandung (BA) and Sutherland (SU). We have seen that the phase had to be reduced of  $30^\circ$  in Europe also to fit the observations. For Canberra (CB) and Tigo/Concepcion (TC) there is nothing in common between the **B** and **L** vectors.

To summarize we can say that the FES04 model seems to fit partly the observations in Eastern Canada (CA) and in Japan (ES and MA). In the Indian Ocean (SU and BA) the phase should be reduced by  $30^\circ$ . Moreover the amplitude is always too small to fit the observations. There is no agreement in Chile (TC) and Australia (CB).

## 6. Conclusions

Tidal loading on M4 frequency is still important at several hundred kilometres inside the continents. The only station without noticeable effect is Boulder (BO). Among 14 constituents listed as non-linear tides by oceanographers we can detect up to 11 constituents in some tidal gravity stations. A few of them only are present in the tidal potential at a level larger than 2ngal at the equator. M4 itself reaches only 27ngal at the equator.

The tidal gravity observations can help to discriminate between different ocean tides models if the distance to the sea is large enough to reduce the influence of the finite grid, which is not able to follow exactly the coast. In Europe the results for M4 points clearly to a better efficiency of the tidal loading corrections computed using the Pingree & Griffiths model. For stations beyond  $10^\circ$  of East longitude, the final residue reaches the level of 1ngal ( $10^{-11}\text{ms}^{-2}$ ) only.

Reasonable tidal factors are obtained in stations (Boulder and Wuhan), where the loading is weak and the theoretical amplitude at the level of 10 ngal. It means that instrumental nonlinearities are not producing spurious signals at M4 frequency.

The M4 tide included in the ocean model FES04 does not provide efficient tidal loading corrections for tidal gravity observations. In Europe, where the shallow water tides are well constrained, the amplitude of the load vector is correct, but there is a  $30^\circ$  phase advance with respect to the observed tidal residues. A similar phase advance seems to exist in the Indian Ocean and the computed amplitude is too low. In Japan and Western Canada the phase is correct but the amplitude is too low. The model is not diminishing the observed residue in Australia (CB) and South America (TC). It is obvious that more detailed local models are required to reach a reasonable agreement between the observations and the modelled ocean tides effect. Western Europe is a good example of such agreement.

The elimination of QD components, including the non-linear tides, from the tidal residues is effective using the VAV tidal analysis program.

## Acknowledgements

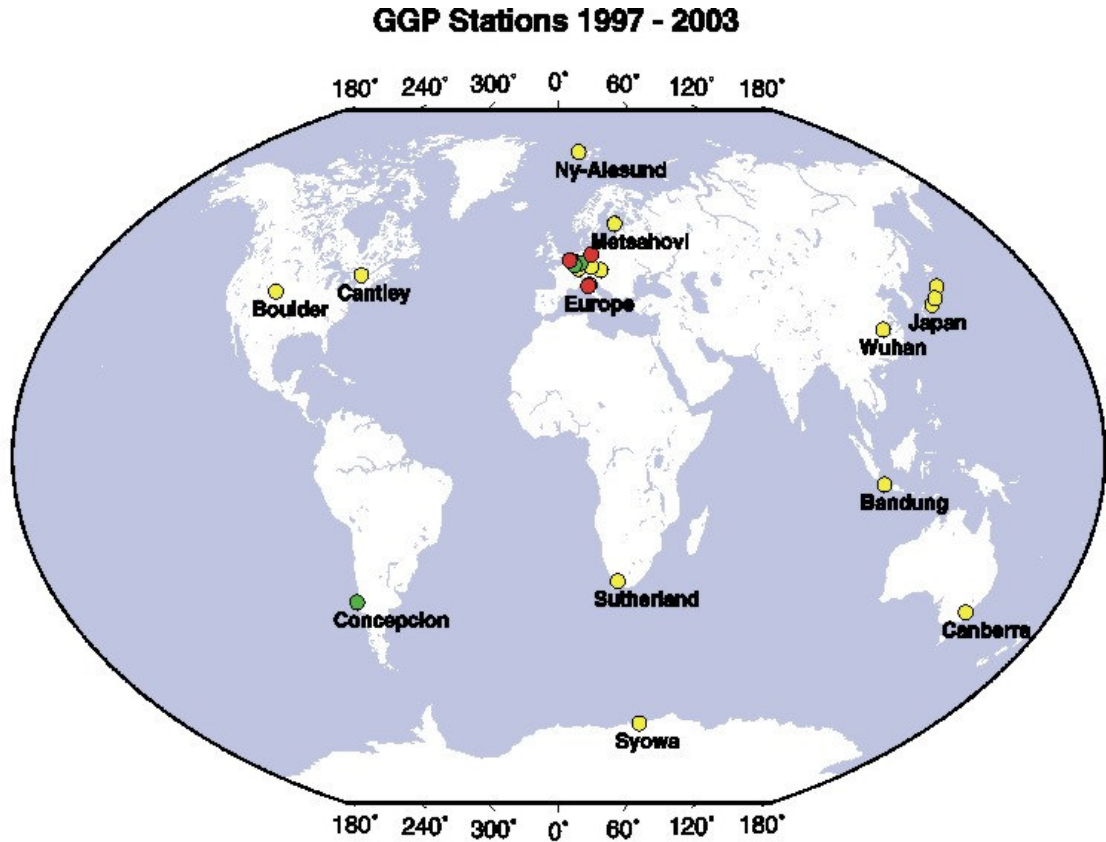
The stay at the Royal Observatory of Belgium of Zhou JiangCun was partly supported by the Bilateral Scientific and Technical Agreements between Belgium and China (project "SG observations and Geodynamics", BL/33/C17), and Sun Heping was partly supported by the knowledge innovation project of Chinese Academy of Sciences (KZCX2-YW-133) and National Natural Sciences Foundation of China (40730316).

## BIBLIOGRAPHY

- Boy, J.-P., Llubes, M., Ray, R., Hinderer, J., Florsch N., Rosat, S., Lyard, F., Letellier, T. (2004). Non-linear oceanic tides observed by superconducting gravimeters in Europe. *Journal of Geodynamics*, 38 (3-5), 391-405.
- Crossley, D., Hinderer, J., Casula, G., Francis, O., Hsu, H. T., Imanishi, Y., Jentzsch, G., Kääriäinen, J., Merriam, J., Meurers, B., Neumeier, J., Richter, B., Shibuya, K., Sato, T., Van Dam, T. (1999). Network of superconducting gravimeters benefits a number of disciplines. *EOS*, 80, 11, 121/125-126.
- Dehant, V., Defraigne, P., Wahr, J. (1999). Tides for a convective Earth. *J. Geoph. Res.*, 104, B1, 1035-1058.
- Ducarme, B., Venedikov, A. P., Arnos, J., Vieira, R. (2006). Analysis and prediction of ocean tides by the computer program VAV. *J. Geodynamics*, 41(1-3), 100-111.
- Farrell, W. E. (1972). Deformation of the Earth by surface load. *Rev. Geophys. Space Phys.*, 10, 761-797.
- Flather, R.A. (1976). A tidal model of the North-West European Continental shelf. *Mém. Soc. R. Oc.; Liège*, 9, 141-164.
- Florsch, N., Hinderer, J., Legros, H. (1995). Identification of quarter-diurnal tidal waves in superconducting gravimeter data. *Bull. Inf. Marées Terrestres*, 122, 9189-9198.
- Pingree, R.D., Maddock, L. (1978). The M4 tide in the English Channel derived from a non-linear numerical model of the M2 tide. *Deep Sea Res.*, 25, 53-63.
- Pingree, R.D., Griffiths, K. D. (1980). Currents driven by a steady uniform windstress on the shelf seas around the British Isles. *Oceanol. Acta*, 3, 227-235.
- Pingree, R.D., Griffiths, K. D. (1981). S2 tidal simulation on the North-West European shelf. *J. Mar. Biol. Assoc., UK* 61, 609-616.
- Sakamoto, Y., Ishiguro, M., Kitagawa, G. (1986). Akaike Information Criterion statistics. *D. Reidel Publishing Company, Tokyo*, 290pp.
- Sun, H.P., Xu, J.Q., Ducarme, B. (2003). Search for the translational triplet of the Earth's solid inner core by SG observations at GGP stations. *Bull. Inf. Marées Terrestres* 138, 10977-10985
- Sun, H.P., Xu, J.Q., Ducarme, B. (2004). Detection of the translational oscillations of the Earth's solid inner core based on the international superconducting gravimeter observations. *Bull. Inf. Marées Terrestres*, 122, 9189-9198.
- Tamura, Y. (1987). An harmonic development of the tide-generating potential. *Bull. Inf. Marées Terrestres*, 99, 6813-6855.

Venedikov, A. P., Arnosó, J., Vieira, R. (2003). VAV: a program for tidal data processing. *Comput. Geosci.*, 29, 487-502.

Venedikov, A. P., Arnosó, J., Vieira, R. (2005). New version of the program VAV for tidal data processing. *Comput. Geosci.*, 31, 667-669.



GMT 2009 Jan 31 10:20:44

Figure 1: Global GGP network

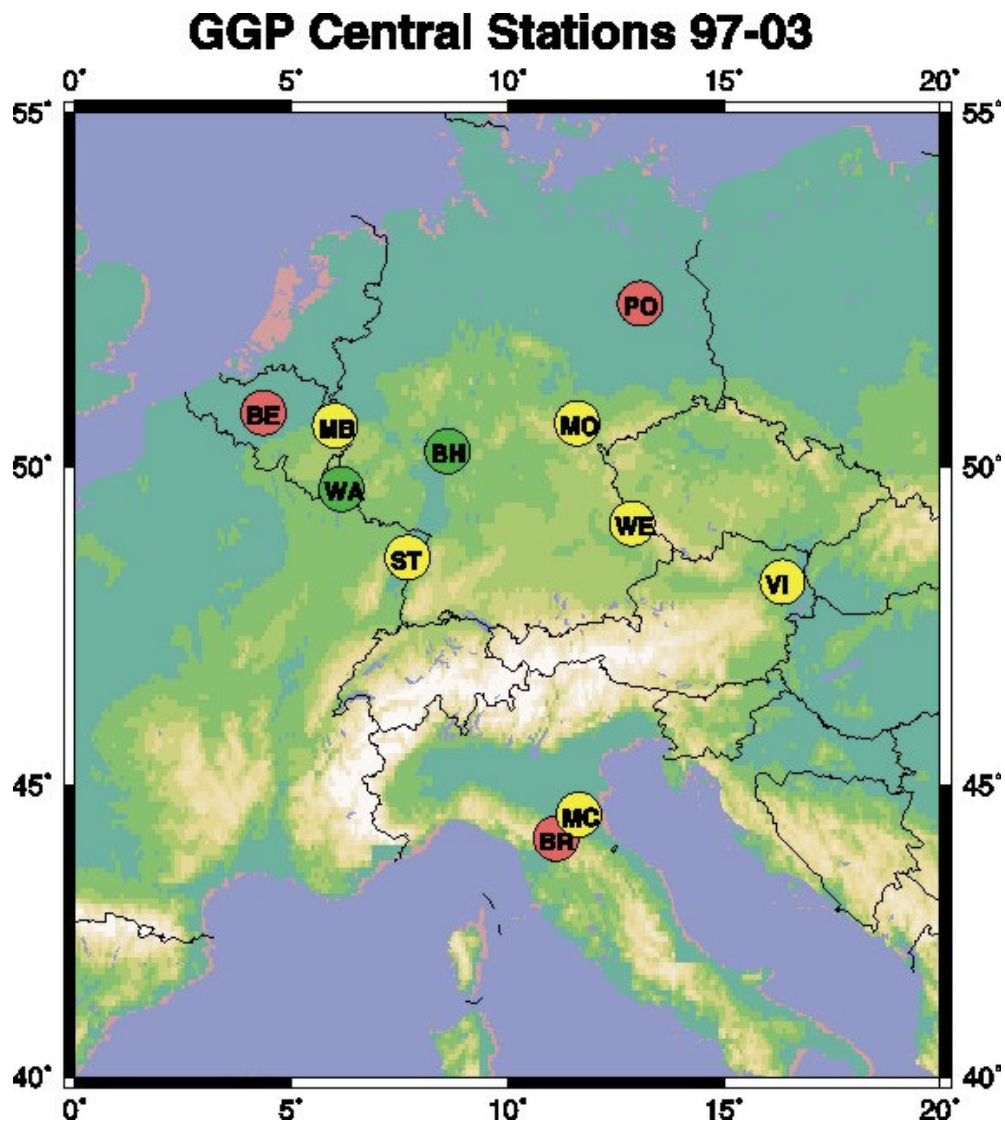


Figure 2: GGP European network

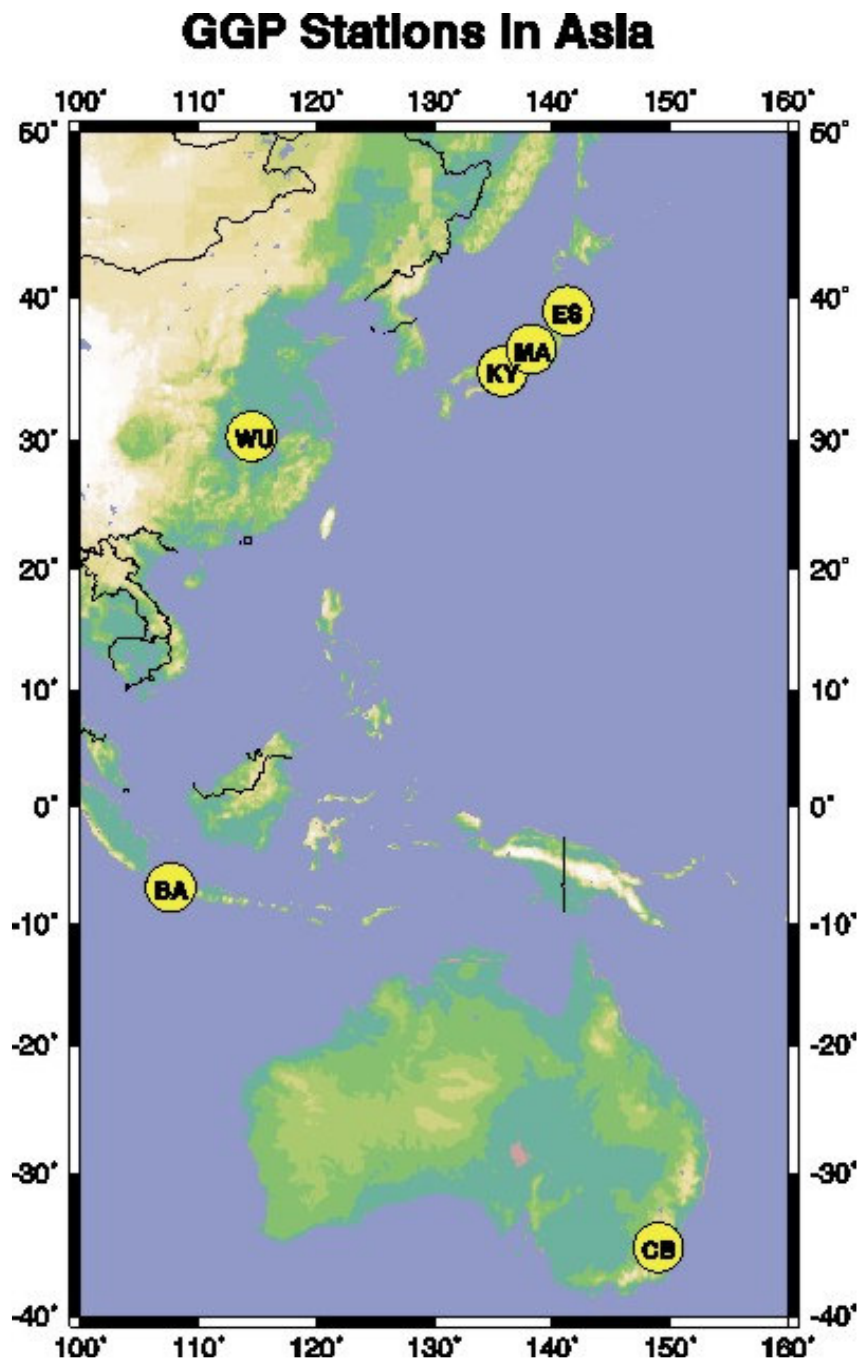


Figure 3: GGP stations in Asia and Australia